

Electric dipole moments: A global analysis

Timothy Chupp

Physics Department, University of Michigan, Ann Arbor, Michigan 48109, USA

Michael Ramsey-Musolf

*Amherst Center for Fundamental Interactions, Department of Physics,**University of Massachusetts–Amherst, Amherst, Massachusetts 01003, USA**and Kellogg Radiation Laboratory, California Institute of Technology, Pasadena, California 91125, USA*

(Received 6 August 2014; published 6 March 2015)

We perform a global analysis of searches for the permanent electric dipole moments (EDMs) of the neutron, neutral atoms, and molecules in terms of six leptonic, semileptonic, and nonleptonic interactions involving photons, electrons, pions, and nucleons. By translating the results into fundamental charge-conjugation-parity symmetry (CP) violating effective interactions through dimension six involving standard model particles, we obtain rough lower bounds on the scale of beyond the standard model CP-violating interactions ranging from 1.5 TeV for the electron EDM to 1300 TeV for the nuclear spin-independent electron-quark interaction. We show that planned future measurements involving systems or combinations of systems with complementary sensitivities to the low-energy parameters may extend the mass reach by an order of magnitude or more.

DOI: [10.1103/PhysRevC.91.035502](https://doi.org/10.1103/PhysRevC.91.035502)

PACS number(s): 11.30.Er, 14.60.Cd, 32.10.Dk, 33.15.Kr

I. INTRODUCTION

The search for permanent electric dipole moments (EDMs) of neutrons, atoms, and molecules provides one of the most powerful probes of the combination of time-reversal (T) and parity (P) symmetry and the underlying combination of charge conjugation (C) and P at the elementary particle level (for recent reviews, see Refs. [1–3]). The nonobservation of the EDMs of the neutron (d_n) [4] and ^{199}Hg atom [5] is consistent with the standard model (SM) CP violation (CPV) characterized by the Cabibbo-Kobayashi-Maskawa (CKM) matrix but implies a vanishingly small coefficient $\bar{\theta}$ of the CPV $G\bar{G}$ operator in the SM strong interaction Lagrangian. Scenarios for physics beyond the standard model (BSM) typically predict the existence of new sources of CPV that—in contrast to the CKM CPV—do not give suppressed contributions to EDMs unless the CPV parameters themselves are small or the mass scales high. The presence of new CPV interactions is required to account for the cosmic matter-antimatter asymmetry. If the associated energy scale is not too high compared to the scale of electroweak symmetry breaking (EWSB), and if the responsible CPV interactions are flavor diagonal, then EDMs provide a particularly important window [6].

The past decade has witnessed tremendous strides in the sensitivity of EDM searches as well as the development of prospects for even more sensitive tests. Recently, the ACME Collaboration [7] has reported a limit on the EDM of the paramagnetic ThO molecule that yields an order of magnitude more stringent bounds on CPV interactions than limits implied by previously reported results from YbF [8] and Tl [9]. As we discuss below, the ACME result probes BSM mass scale Λ ranging from 1.5 TeV for the electron EDM to 1300 TeV for the nuclear spin-independent electron-quark interaction. A few years earlier, a similar advance in sensitivity was achieved for $d_A(^{199}\text{Hg})$ [5]. Looking to the future, efforts are under way to improve the sensitivity of d_n searches by one to two orders of magnitude, to achieve similar progress in neutral atoms such

as Xe, Rn, and Ra, and to explore the development of proton and light nuclear EDM searches using storage rings (for a recent discussion of present and future EDM search efforts, see Ref. [10]). For $O(1)$ BSM CPV phases, these experiments could probe Λ of order 50–100 TeV.

In this context, it is useful to try and develop a global picture of the information that has been or will be provided by present and future EDM searches. Ideally, one would like to interpret the results in terms of underlying BSM interactions in a way that would point in the direction of, or rule out, particular scenarios for new CPV. In practice, most analyses follow a more constrained approach. Theorists often work within the framework of a specific model, such as the minimal supersymmetric standard model, and derive constraints on the model parameters from the EDM search null results (see, e.g., Refs. [11,12]). Experimental analyses, on the other hand, are often agnostic about a specific model realization but report limits on various “sources” of an EDM (e.g., the quark EDM or chromo-EDM; see below), assuming only one of these is present. While entirely appropriate, such studies inherently either build in a model-dependent bias or preclude the possibility that multiple sources may be present and, thus, may not reveal the full landscape of CPV sources probed by EDM experiments. For these reasons, it is also instructive to consider EDMs from a model-independent perspective that does not impose the “single-source” restriction.

In what follows, we begin this undertaking by providing a model-independent, global analysis of EDM searches. We carry out this analysis in terms of a set of low-energy hadronic and atomic parameters that one may ultimately match onto CPV interactions at the elementary particle level. It is particularly convenient to organize the latter in terms of an effective field theory (EFT) involving standard model degrees of freedom. The effective operators arising in the EFT constitute the CPV “sources.” In this context, the EFT provides a bridge between the atomic, nuclear, and hadronic

matrix elements most directly related to the EDM searches and the possible origins of new CPV involving BSM particles and their interactions. A given BSM scenario will yield specific, model-dependent predictions for the EFT operator coefficients that one may compare with the constraints obtained from our model-independent global analysis. A detailed discussion of the EFT and its relation to both the low-energy parameters and various BSM scenarios appears in Ref. [1], whose notation and logic we generally adopt in this paper.

The atomic, molecular, hadronic, and nuclear matrix elements most directly related to the experimental EDMs themselves arise from a set of low-energy leptonic, semileptonic, and nonleptonic interactions. As we discuss below, the dominant contributions arise from d_e ; T- and P-violating (TVPV)¹ pseudoscalar-scalar and tensor electron-nucleon interactions, characterized by strengths C_S and C_T , respectively; the isoscalar and isovector TVPV pion-nucleon couplings $\bar{g}_\pi^{(I)}$ for $I = 0, 1$; and a “short-distance” contribution to the neutron EDM, \bar{d}_n^{sr} (denoted simply “ \bar{d}_n ” in Ref. [1]). In this context, we find the following:

- (i) The EDMs of paramagnetic systems are primarily sensitive to d_e and C_S . Inclusion of both d_e and C_S in the global fit yields an upper bound on each parameter that is an order of magnitude less stringent than would be obtained under the “single-source” assumption.²
- (ii) Diamagnetic atom EDMs carry the strongest sensitivity to C_T and the $\bar{g}_\pi^{(0,1)}$, whereas the neutron EDM depends most strongly on \bar{d}_n^{sr} and $\bar{g}_\pi^{(0)}$, providing four effective CPV parameters that are constrained by results from four experimental systems.
- (iii) Uncertainties in the nuclear theory preclude extraction of a significant limit on $\bar{g}_\pi^{(1)}$ from d_A (¹⁹⁹Hg), whereas the situation regarding $\bar{g}_\pi^{(0)}$ is under better theoretical control. Including the TIF and ¹²⁹Xe in the global fit leads to an order of magnitude tighter constraint on $\bar{g}_\pi^{(1)}$ than on $\bar{g}_\pi^{(0)}$.
- (iv) Looking to the future, a new probe of the alkali-metal (e.g., Cs or Fr) EDM with a d_e sensitivity of 10^{-28} e cm [16] could have a significantly stronger impact on the combined $d_e - C_S$ global fit than would an order of magnitude improvement in the ThO sensitivity. The addition of new, more stringent limits on the EDMs of the neutron, ¹²⁹Xe atom, and ²²⁵Ra or Rn atom would lead to substantial improvements in the sensitivities to both $\bar{g}_\pi^{(0)}$ and $\bar{g}_\pi^{(1)}$.

The quantitative implications of these features are summarized in Table I, where we present our results for 95% confidence-level upper limits based on the current set of experimental results.

¹The symmetry violation studied experimentally is explicitly TVPV, rather than CPV, as the systems consist of only particles and not their antiparticles. By virtue of the CPT theorem, these observables are related to CPV interactions and the elementary particle level, assuming the latter are described by a relativistic quantum field theory.

²This has been discussed by other authors, for example, in Refs. [3,13–15].

TABLE I. Ninety-five percent confidence level bounds on the six parameters characterizing the EDMs of the neutrons, neutral atoms, and molecules obtained from the fit described in the text.

Parameter (units)	95% limit
d_e (e cm)	5.4×10^{-27}
C_S	4.5×10^{-7}
C_T	2×10^{-6}
\bar{d}_n^{sr} (e cm)	12×10^{-23}
$\bar{g}_\pi^{(0)}$	8×10^{-9}
$\bar{g}_\pi^{(1)}$	1×10^{-9}

In terms of the underlying CPV sources, it is interesting to discuss the significance of the foregoing. Among the highlights are the following:

- (i) The QCD parameter $\bar{\theta}$ enters most strongly through $\bar{g}_\pi^{(0)}$ and \bar{d}_n^{sr} . From Table I and the analysis of hadronic matrix elements in Ref. [1], we conclude that $|\bar{\theta}| \leq \bar{\theta}_{\text{max}}$ with $2 \times 10^{-7} \lesssim \bar{\theta}_{\text{max}} \lesssim 1.6 \times 10^{-6}$, where the bound is dominated by the constraint on $\bar{g}_\pi^{(0)}$ and where the range is associated with the theoretical, hadronic physics uncertainty. We observe that this limit is considerably weaker than would be obtained under the “single-source” assumption.
- (ii) The quantities d_e and C_S are most naturally expressed in terms of $(v/\Lambda)^2$, where $v = 246$ GeV is the weak scale; the electron Yukawa coupling Y_e ; and a set of dimensionless Wilson coefficients δ_e and $C_{\text{eq}}^{(-)}$. Since the electron EDM is a dipole operator, it carries one power of Y_e whereas the semileptonic interaction does not. For a given value of the BSM scale Λ , the results in Table I imply a constraint on $C_{\text{eq}}^{(-)}$ that is roughly five hundred times more stringent than the bound on δ_e . In the event that $C_{\text{eq}}^{(-)}$ and δ_e arise at tree-level and one-loop orders, respectively, the corresponding lower bound on Λ from C_S is roughly a thousand times greater than the limit extracted from d_e . Thus, for BSM scenarios that generate both a nonvanishing $C_{\text{eq}}^{(-)}$ and δ_e , the impact of the semileptonic CPV interaction on paramagnetic atom EDMs may be considerably more pronounced than that of the electron EDM.
- (iii) The bounds on $\bar{g}_\pi^{(1)}$ are roughly ten times weaker than quoted in earlier theoretical literature, owing in part to use of a theoretically consistent computation of its contribution to the neutron EDM [17]. For some underlying CPV sources, such as those generated in left-right symmetric models, the dependence of diamagnetic-atom EDMs on $\bar{g}_\pi^{(1)}$ may be relatively more important than the dependence on $\bar{g}_\pi^{(0)}$ due to an isospin-breaking suppression of the latter. Consequently, one may expect more relaxed constraints on CPV parameters in left-right symmetric extensions of the standard model (as well as scenarios that yield sizable isovector quark chromo-EDMs) than previously realized, given the less stringent bounds on $\bar{g}_\pi^{(1)}$.

In the remainder of this paper, we discuss in detail the analysis leading to these conclusions. In Sec. II, we summarize the theoretical framework, drawing largely on the study in Ref. [1]. Section III summarizes the present experimental situation and future prospects. We discuss the observables and their dependence on the six parameters in Table I. In Sec. III A we present the details of our fitting procedure. We conclude with an outlook and discussion of the implications in Sec. IV.

II. THEORETICAL FRAMEWORK

A. Low-energy parameters

The starting point for our analysis is the set of low-energy atomic and hadronic interactions most directly related to the EDM measurements. We distinguish two classes of systems: paramagnetic systems, namely those having an unpaired electron spin, and diamagnetic systems, or those having no unpaired electron (including the neutron).

1. Paramagnetic systems

The EDM response of paramagnetic atoms and polar molecules is dominated by the electron EDM and the nuclear spin-independent (NSID) electron-nucleon interaction. The EDM interaction for an elementary fermion is

$$\mathcal{L}^{\text{EDM}} = -i \sum_f \frac{d_f}{2} \bar{f} \sigma^{\mu\nu} \gamma_5 f F_{\mu\nu}, \quad (2.1)$$

where $F_{\mu\nu}$ is the electromagnetic field strength. In the nonrelativistic limit, Eq. (2.1) contains the TVPV interaction with the electric field \vec{E} ,

$$\mathcal{L}^{\text{EDM}} \rightarrow \sum_f d_f \chi_f^\dagger \vec{\sigma} \chi_f \cdot \vec{E}, \quad (2.2)$$

where χ_f is the Pauli spinor for fermion f and $\vec{\sigma}$ is the vector of Pauli matrices. The NSID interaction has the form

$$\mathcal{L}_{eN}^{\text{NSID}} = -\frac{G_F}{\sqrt{2}} \bar{e} i \gamma_5 e \bar{N} [C_S^{(0)} + C_S^{(1)} \tau_3] N, \quad (2.3)$$

where G_F is the Fermi constant, N is a nucleon spinor and τ_3 is the nucleon isospin Pauli matrix. Taking the nuclear matrix element assuming nonrelativistic nucleons leads to the atomic Hamiltonian

$$\hat{H}_S = \frac{iG_F}{\sqrt{2}} \delta(\vec{r}) [(Z+N)C_S^{(0)} + (Z-N)C_S^{(1)}] \gamma_0 \gamma_5, \quad (2.4)$$

where a sum over all nucleons is implied, and where the Dirac matrices act on the electron wave function. The resulting atomic EDM d_A is then given by

$$d_A = \rho_A^e d_e - \kappa_S^{(0)} C_S, \quad (2.5)$$

where

$$C_S \equiv C_S^{(0)} + \left(\frac{Z-N}{Z+N} \right) C_S^{(1)} \quad (2.6)$$

and where ρ_A^e and $\kappa_S^{(0)}$ are obtained from atomic and hadronic computations. For polar molecules, the effective Hamiltonian is

$$\hat{H}_{\text{mol}} = [W_d d_e + W_S (Z+N)C_S] \vec{S} \cdot \hat{n} + \dots, \quad (2.7)$$

where \vec{S} and \hat{n} denote the unpaired electron spin and unit vector along the intermolecular axis, respectively. The quantities W_d and W_S that give the sensitivities of the molecular energy to the electron EDM and electron-quark interaction are obtained from molecular structure calculations [18,19,39]. The resulting ground-state (g.s.) matrix element in the presence of an external electric field \vec{E}_{ext} is

$$\langle \text{g.s.} | \hat{H}_{\text{mol}} | \text{g.s.} \rangle = [W_d d_e + W_S (Z+N)C_S] \eta(E_{\text{ext}}) \quad (2.8)$$

with

$$\eta(E_{\text{ext}}) = \langle \text{g.s.} | \vec{S} \cdot \hat{n} | \text{g.s.} \rangle_{E_{\text{ext}}}. \quad (2.9)$$

This takes into account the orientation of the internuclear axis and the internal electric field with respect to the external field, i.e., the electric polarizability of the molecule.

2. Diamagnetic atoms and nucleons

The EDMs of diamagnetic atoms of present experimental interest arise from the nuclear Schiff moment, the individual nucleon EDMs, and the nuclear-spin-dependent electron-nucleon interaction. We define the latter as

$$\mathcal{L}_{eN}^{\text{NSD}} = \frac{8G_F}{\sqrt{2}} \bar{e} \sigma_{\mu\nu} e v^\nu \bar{N} [C_T^{(0)} + C_T^{(1)} \tau_3] S^\mu N + \dots, \quad (2.10)$$

where S^μ is the spin of a nucleon moving with velocity v^μ and where the $+\dots$ indicates subleading contributions arising from the electron scalar \times nucleon pseudoscalar interaction. The resulting Hamiltonian is

$$\hat{H}_T = \frac{2iG_F}{\sqrt{2}} \delta(\vec{r}) [C_T^{(0)} + C_T^{(1)} \tau_3] \vec{\sigma}_N \cdot \vec{\gamma}, \quad (2.11)$$

where a sum over all nucleons is again implicit; $\vec{\sigma}_N$ is the nucleon spin Pauli matrix, and $\vec{\gamma}$ acts on the electron wave function. Including the effect of \hat{H}_T , the individual nucleon EDMs d_N , and the nuclear Schiff moment S , one has

$$d_A = \sum_{N=p,n} \rho_Z^N d_N + \kappa_S S - [k_T^{(0)} C_T^{(0)} + k_T^{(1)} C_T^{(1)}], \quad (2.12)$$

where $k_T^{(0,1)}$ give the sensitivities of the atomic EDM to the isoscalar and isovector electron-quark tensor interactions. A compilation of the ρ_Z^N , κ_S , and $k_T^{(0,1)}$ can be found in Ref. [1].³

The nuclear Schiff moment arises from a TVPV nucleon-nucleon interaction generated by pion exchange, where one of the pion-nucleon vertices is the strong pion-nucleon coupling and the other is the TVPV pion-nucleon interaction:

$$\mathcal{L}_{\pi NN}^{\text{TVPV}} = \bar{N} [\bar{g}_\pi^{(0)} \vec{\tau} \cdot \vec{\pi} + \bar{g}_\pi^{(1)} \pi^0 + \bar{g}_\pi^{(2)} (3\tau_3 \pi^0 - \vec{\tau} \cdot \vec{\pi})] N. \quad (2.13)$$

As discussed in detail in Ref. [1] and references therein, the isotensor coupling $\bar{g}_\pi^{(2)}$ is generically suppressed by a factor $\lesssim 0.01$ with respect to $\bar{g}_\pi^{(0)}$ and $\bar{g}_\pi^{(1)}$ by factors associated with isospin breaking and/or the electromagnetic interaction for

³We note that the values for the κ_S given in that work should be multiplied by an overall factor of -1 given the convention used there and in Eq. (2.12).

underlying sources of CPV. Consequently we will omit $\bar{g}_\pi^{(2)}$ from our analysis. The nuclear Schiff moment can then be expressed as

$$S = \frac{m_N g_A}{F_\pi} [a_0 \bar{g}_\pi^{(0)} + a_1 \bar{g}_\pi^{(1)}], \quad (2.14)$$

where $g_A \approx 1.27$ is the nucleon isovector axial coupling, and $F_\pi = 92.4 \text{ MeV}$ is the pion decay constant. The specific values of $a_{0,1}$ for the nuclei of interest are tabulated in Table VI. As discussed in detail in Ref. [1], there exists considerable uncertainty in the nuclear Schiff moment calculations, so we will adopt the “best values” and theoretical ranges for the $a_{0,1}$ given in that work.

The neutron and proton EDMs arise from two sources. The long-range contributions from the TVPV π - NN interaction have been computed using heavy baryon chiral perturbation theory, with the remaining short-distance contributions contained in the “low-energy constants” \bar{d}_n^{sr} and \bar{d}_p^{sr} [17]:

$$d_n = \bar{d}_n^{\text{sr}} - \frac{e g_A \bar{g}_\pi^{(0)}}{8\pi^2 F_\pi} \left\{ \ln \frac{m_\pi^2}{m_N^2} - \frac{\pi m_\pi}{2m_N} + \frac{\bar{g}_\pi^{(1)}}{4\bar{g}_\pi^{(0)}} (\kappa_1 - \kappa_0) \frac{m_\pi^2}{m_N^2} \ln \frac{m_\pi^2}{m_N^2} \right\}, \quad (2.15)$$

$$d_p = \bar{d}_p^{\text{sr}} + \frac{e g_A \bar{g}_\pi^{(0)}}{8\pi^2 F_\pi} \left\{ \ln \frac{m_\pi^2}{m_N^2} - \frac{2\pi m_\pi}{m_N} - \frac{\bar{g}_\pi^{(1)}}{4\bar{g}_\pi^{(0)}} \left[\frac{2\pi m_\pi}{m_N} + \left(\frac{5}{2} + \kappa_0 + \kappa_1 \right) \frac{m_\pi^2}{m_N^2} \ln \frac{m_\pi^2}{m_N^2} \right] \right\}, \quad (2.16)$$

where κ_0 and κ_1 are the isoscalar and isovector nucleon anomalous magnetic moments, respectively. At present, we do not possess an up-to-date, consistent set of ρ_Z^N for all of the diamagnetic atoms of interest here. Rather than introduce an additional set of associated nuclear theory uncertainties, we do not include these terms in our fit. Looking to the future, additional nuclear theory work in this regard would be advantageous since, for example, the sensitivity of the present ^{199}Hg result to d_n is not too different from the direct limit [4].

3. Low-energy parameters: summary

Based on the foregoing discussion, our global analysis of EDM searches will take into account the following parameters:

- (i) d_e and C_S for paramagnetic atoms and polar molecules.
- (ii) $\bar{g}_\pi^{(0)}$, $\bar{g}_\pi^{(1)}$, C_T , and \bar{d}_n^{sr} for diamagnetic systems and the neutron.

B. CPV sources of the low-energy parameters

In order to interpret the low-energy parameters in terms of underlying sources of CPV, we will consider those contained in the SM as well as possible physics beyond the SM. A convenient, model-independent framework for doing so entails writing the CPV Lagrangian in terms of SM fields [1]:

$$\mathcal{L}_{\text{CPV}} = \mathcal{L}_{\text{CKM}} + \mathcal{L}_{\bar{\theta}} + \mathcal{L}_{\text{BSM}}^{\text{eff}}. \quad (2.17)$$

TABLE II. Dimension-six CPV operators that induce atomic, hadronic, and nuclear EDMs. Here φ is the SM Higgs doublet, $\tilde{\varphi} = i\tau_2 \varphi^*$, and $\Phi = \varphi(\tilde{\varphi})$ for $I_f < 0$ (> 0).

$\mathcal{O}_{\tilde{G}}$	$f^{ABC} \tilde{G}_\mu^{Av} G_\nu^{B\rho} G_\rho^{C\mu}$	CPV 3 gluon
\mathcal{O}_{uG}	$(\tilde{Q}^{\sigma\mu\nu} T^A u_R) \tilde{\varphi} G_{\mu\nu}^A$	Up-quark chromo EDM
\mathcal{O}_{dG}	$(\tilde{Q}^{\sigma\mu\nu} T^A d_R) \varphi G_{\mu\nu}^A$	Down-quark chromo EDM
\mathcal{O}_{fW}	$(\tilde{F}^{\sigma\mu\nu} f_R) \tau^I \Phi W_{\mu\nu}^I$	Fermion $\text{SU}(2)_L$ weak dipole
\mathcal{O}_{fB}	$(\tilde{F}^{\sigma\mu\nu} f_R) \Phi B_{\mu\nu}$	Fermion $\text{U}(1)_Y$ weak dipole
$\mathcal{Q}_{le dq}$	$(\tilde{L}^j e_R) (\tilde{d}_R Q^j)$	CPV semileptonic
$\mathcal{Q}_{le qu}^{(1)}$	$(\tilde{L}^j e_R) \epsilon_{jk} (\tilde{Q}^k u_R)$	
$\mathcal{Q}_{le qu}^{(3)}$	$(\tilde{L}^j \sigma_{\mu\nu} e_R) \epsilon_{jk} (\tilde{Q}^k \sigma^{\mu\nu} u_R)$	
$\mathcal{Q}_{quqd}^{(1)}$	$(\tilde{Q}^j u_R) \epsilon_{jk} (\tilde{Q}^k d_R)$	CPV four quark
$\mathcal{Q}_{quqd}^{(8)}$	$(\tilde{Q}^j T^A u_R) \epsilon_{jk} (\tilde{Q}^k T^A d_R)$	
$\mathcal{Q}_{qu d}$	$i(\tilde{\varphi}^\dagger D_\mu \varphi) \bar{u}_R \gamma^\mu d_R$	Quark-Higgs

Here the CPV SM CKM [21] and QCD [22–24] interactions are

$$\mathcal{L}_{\text{CKM}} = -\frac{ig_2}{\sqrt{2}} V_{\text{CKM}}^{pq} \bar{U}_L^p W^+ D_L^q + \text{H.c.}, \quad (2.18)$$

$$\mathcal{L}_{\bar{\theta}} = -\frac{g_3^2}{16\pi^2} \bar{\theta} \text{Tr}(G^{\mu\nu} \tilde{G}_{\mu\nu}), \quad (2.19)$$

where g_2 and g_3 are the weak and strong coupling constants, respectively, U_L^p (D_L^p) is a generation- p ($p = 1, 2, 3$) left-handed up-type (down-type) quark field, V_{CKM}^{pq} denotes a CKM matrix element, W_μ^\pm are the charged weak gauge fields, and $\tilde{G}_{\mu\nu} = \epsilon_{\mu\nu\alpha\beta} G^{\alpha\beta} / 2$ ($\epsilon_{0123} = 1$)⁴ is the dual to the gluon field strength $G^{\mu\nu}$. The effects of possible BSM CPV are encoded in a tower of higher-dimension effective operators,

$$\mathcal{L}_{\text{BSM}}^{\text{eff}} = \frac{1}{\Lambda^2} \sum_i \alpha_i^{(6)} \mathcal{O}_i^{(6)} + \dots, \quad (2.20)$$

where Λ is the BSM mass scale considered to lie above the weak scale $v = 246 \text{ GeV}$, and where we have shown explicitly only those operators arising at dimension six. These operators [25] are listed in Tables 3 and 4 of Ref. [1]. For purposes of this review, we focus on the subset listed in Table II.

After EWSB, quark-gluon interactions give rise to the quark chromoelectric dipole moment (CEDM) interaction:

$$\mathcal{L}^{\text{CEDM}} = -i \sum_q \frac{g_3 \tilde{d}_q}{2} \bar{q} \sigma^{\mu\nu} T^A \gamma_5 q G_{\mu\nu}^A, \quad (2.21)$$

where T^A ($A = 1, \dots, 8$) are the generators of the color group. Analogously, \mathcal{Q}_{fW} and \mathcal{Q}_{fB} generate the elementary fermion EDM interactions of Eq. (2.1). Letting

$$\alpha_{fV_k}^{(6)} \equiv g_k C_{fV_k}, \quad (2.22)$$

⁴Note that our sign convention for $\epsilon_{\mu\nu\alpha\beta}$, which follows that of Ref. [25], is opposite to what is used in Ref. [3] and elsewhere. Consequently, $\mathcal{L}_{\bar{\theta}}$ carries an overall -1 compared to what frequently appears in the literature.

where $V_k = B, W,$ and G for $k = 1, 2, 3$ respectively; the relationships between the \tilde{d}_q and d_f and the C_{fV_k} are

$$\tilde{d}_q = -\frac{\sqrt{2}}{v} \left(\frac{v}{\Lambda}\right)^2 \text{Im } C_{qG}, \quad (2.23)$$

$$d_f = -\frac{\sqrt{2}e}{v} \left(\frac{v}{\Lambda}\right)^2 \text{Im } C_{f\gamma}, \quad (2.24)$$

where

$$\text{Im } C_{f\gamma} \equiv \text{Im } C_{fB} + 2I_3^f \text{Im } C_{fW}; \quad (2.25)$$

and I_3^f is the third component of weak isospin for fermion f . Here, we have expressed d_f and \tilde{d}_q in terms of the Fermi scale $1/v$, a dimensionless ratio involving the BSM scale Λ and v , and the dimensionless Wilson coefficients. Expressing these quantities in units of fm one has

$$\tilde{d}_q = -(1.13 \times 10^{-3} \text{ fm}) \left(\frac{v}{\Lambda}\right)^2 \text{Im } C_{qG}, \quad (2.26)$$

$$d_f = -(1.13 \times 10^{-3} e \text{ fm}) \left(\frac{v}{\Lambda}\right)^2 \text{Im } C_{f\gamma}. \quad (2.27)$$

As discussed in Ref. [1], it is useful to observe that the EDM and CEDM operator coefficients are typically proportional to the corresponding fermion masses,⁵ as the operators that generate them above the weak scale ($Q_{q\tilde{G}}, Q_{f\tilde{W}}, Q_{f\tilde{B}}$) contain explicit factors of the Higgs field dictated by electroweak gauge invariance. It is thus convenient to make the dependence on the corresponding fermion Yukawa couplings $Y_f = \sqrt{2}m_f/v$ explicit and to define two dimensionless quantities δ_q and δ_f that embody all of the model-specific dynamics responsible for the EDM and CEDM, respectively, apart from Yukawa insertion:

$$\text{Im } C_{qG} \equiv Y_q \tilde{\delta}_q \rightarrow \tilde{d}_q = -(1.13 \times 10^{-3} \text{ fm}) \left(\frac{v}{\Lambda}\right)^2 Y_q \tilde{\delta}_q, \quad (2.28)$$

$$\text{Im } C_{f\gamma} \equiv Y_f \delta_f \rightarrow d_f = -(1.13 \times 10^{-3} e \text{ fm}) \left(\frac{v}{\Lambda}\right)^2 Y_f \delta_f. \quad (2.29)$$

While one often finds bounds on the elementary fermion EDM and CEDMs quoted in terms of d_f and \tilde{d}_q , the quantities δ_f and $\tilde{\delta}_q$ are typically more appropriate when comparing with the Wilson coefficients of other dimension-six CPV operators (see below). One may also derive generic (though not airtight) expectations for the relative magnitudes of various dipole operators. For example, for a BSM scenario that generates both quark and lepton EDMs and that does not discriminate between them apart from the Yukawa couplings, one would expect $\delta_q \sim \delta_\ell$. On the other hand, the corresponding light quark EDM d_q would be roughly an order of magnitude larger than that of the electron, given the larger (by a factor of ten) light

quark Yukawa coupling.⁶ In what follows, we will therefore quote constraints on both d_e and δ_e implied by results for paramagnetic systems; for implications of the neutron and diamagnetic results for the quark EDMs (d_q/δ_q) and CEDMs ($\tilde{d}_q/\tilde{\delta}_q$) we refer the reader to Ref. [1].

The remaining operators in Table II include $O_{\tilde{G}}$, the CPV Weinberg three-gluon operator (sometimes called the gluon CEDM); a set of three semileptonic operators $Q_{ledq}, Q_{lequ}^{(1)}, Q_{lequ}^{(3)}$; and two four-quark operators $Q_{quqd}^{(1)}$ and $Q_{quqd}^{(8)}$. An additional four-quark CPV interaction arises from the quark-Higgs operator $Q_{\phi ud}$ in Table II. After EWSB, this operator contains a $W_\mu^+ \bar{u}_R \gamma^\mu d_R$ vertex that, combined with tree-level exchange of the W boson, gives rise to a CPV $\bar{u}_R \gamma^\mu d_R \bar{d}_L \gamma_\mu u_R$ effective interaction. As a concrete illustration, a nonvanishing Wilson coefficient $\text{Im}C_{\phi ud}$ naturally arises in left-right symmetric models wherein new CPV phases enter via mixing of the left- and right-handed W bosons and through the rotations of the left- and right-handed quarks from the weak to mass eigenstate basis.

The aforementioned operators will give rise to various low-energy parameters of interest to our analysis. Here we summarize a few salient features:

- (i) \mathcal{L}_{CKM} : At the elementary particle level, the CKM-induced quark EDMs vanish through two-loop order; the first nonzero contributions arise at three-loop order for the quarks and four-loop order for the leptons. The effects of elementary fermion EDMs in the hadronic, atomic, and molecular systems of interest here are thus highly suppressed. The dominant CKM contribution enters the neutron EDM and nuclear Schiff moments via the induced CPV penguin operators that generate TVPV strangeness changing meson-nucleon couplings. The expected magnitudes of d_n and diamagnetic-atom EDMs are well below the expected sensitivities of upcoming experiments, so we will not consider the effects of \mathcal{L}_{CKM} further here.
- (ii) $\mathcal{L}_{\bar{\theta}}$: The QCD θ term will directly induce a nucleon EDM as well as the TVPV coupling $\bar{g}_\pi^{(0)}$ at leading order. Since one may rotate away θ when either of the light quark masses vanishes, the contributions of $\bar{\theta}$ to d_n and $\bar{g}_\pi^{(0)}$ are proportional to the square of the pion mass m_π^2 . Chiral symmetry considerations imply that the effect on $\bar{g}_\pi^{(1)}$ and $\bar{g}_\pi^{(2)}$ is suppressed by an additional power of m_π^2 while $\bar{g}_\pi^{(2)}$ is further reduced by the presence of isospin breaking.
- (iii) $\mathcal{L}_{\text{BSM}}^{\text{eff}}$: The presence of the quark CEDM, three-gluon operator, and CPV four-quark operators will induce nonvanishing nucleon EDMs. As noted in Sec. II A the expected magnitude of $\bar{g}_\pi^{(2)}$ relative to $\bar{g}_\pi^{(0)}$ and $\bar{g}_\pi^{(1)}$ is always suppressed by a factor $\lesssim 0.01$ associated with isospin breaking and only the CPV π - NN coupling constants $\bar{g}_\pi^{(0)}$ and $\bar{g}_\pi^{(1)}$ are included in our analysis. Additionally, the effect of a nonvanishing $\text{Im}C_{\phi ud}$ will

⁵Exceptions to this statement do occur.

⁶We will neglect the light-quark mass splitting and replace $Y_u, Y_d \rightarrow Y_q \equiv \frac{\sqrt{2}\bar{m}}{v}$ with \bar{m} being the average light quark mass.

generate both a nucleon EDM and, to leading order in chiral counting, contribute to $\bar{g}_\pi^{(1)}$. As indicated by Eq. (2.15) the long-range contribution to d_n associated with $\bar{g}_\pi^{(1)}$ is suppressed by m_π^2/m_N^2 , whereas the effect on d_p appears at one order lower in m_π/m_N . For the diamagnetic atoms, the nuclear theory uncertainties associated with the $\bar{g}_\pi^{(1)}$ contribution to the ^{199}Hg Schiff moment are particularly large. At present, the sign of a_1 is undetermined, and it is possible that its magnitude may be vanishingly small [1]. In contrast, the computations of a_1 for other diamagnetic systems appear to be on firmer ground.

- (iv) The semileptonic operators O_{ledq} and $O_{lequ}^{(1,3)}$ will induce an effective nucleon spin-independent (NSID) electron-nucleon interaction. The coefficients $C_S^{(0,1)}$ can be expressed in terms of the underlying semileptonic operator coefficients and the nucleon scalar form factors:

$$\begin{aligned} C_S^{(0)} &= -g_S^{(0)} \left(\frac{v}{\Lambda}\right)^2 \text{Im } C_{\text{eq}}^{(-)}, \\ C_S^{(1)} &= g_S^{(1)} \left(\frac{v}{\Lambda}\right)^2 \text{Im } C_{\text{eq}}^{(+)}, \\ C_T^{(0)} &= -g_T^{(0)} \left(\frac{v}{\Lambda}\right)^2 \text{Im } C_{lequ}^{(3)}, \\ C_T^{(1)} &= -g_T^{(1)} \left(\frac{v}{\Lambda}\right)^2 \text{Im } C_{lequ}^{(3)}, \end{aligned} \quad (2.30)$$

where

$$C_{\text{eq}}^{(\pm)} = C_{ledq} \pm C_{lequ}^{(1)}, \quad (2.31)$$

and the isoscalar and isovector form factors $g_\Gamma^{(0,1)}$ are given by

$$\frac{1}{2} \langle N | [\bar{u}\Gamma u + \bar{d}\Gamma d] | N \rangle \equiv g_\Gamma^{(0)} \bar{\psi}_N \Gamma \psi_N, \quad (2.32)$$

$$\frac{1}{2} \langle N | [\bar{u}\Gamma u - \bar{d}\Gamma d] | N \rangle \equiv g_\Gamma^{(1)} \bar{\psi}_N \Gamma \tau_3 \psi_N, \quad (2.33)$$

where $\Gamma = 1$ and $\sigma_{\mu\nu}$, respectively. Values for these form factors can be obtained from Ref. [1].

- (v) We observe that there exist more CPV sources than independent low-energy observables. By restricting one's attention to interactions of mass dimension six or less involving only the first-generation fermions and massless gauge bosons, one finds thirteen independent operators. For the paramagnetic systems, the situation is somewhat simplified, as there exist only three relevant operators: the electron EDM and the two scalar (quark) \times pseudoscalar (electron) interactions. For the systems of experimental interest, the electron EDM and $C_S^{(0)}$ operators dominate. For the diamagnetic systems, on the other hand, there exist ten underlying CPV sources that may give rise to the quantities $\bar{g}_\pi^{(0)}$, $\bar{g}_\pi^{(1)}$, \bar{d}_n^{sr} , and $C_T^{(0,1)}$. Even with the possible addition of a future proton EDM constraint, thereby adding one additional low-energy parameter \bar{d}_p^{sr} , it would not be possible to disentangle all ten sources from the experimentally accessible quantities. Future searches

for the EDMs of light nuclei may provide additional handles (see, e.g., Ref. [1] and references therein), but an analysis of the prospects goes beyond the scope of the present study. Instead, we concentrate on the present and prospective constraints on the dominant low-energy parameters d_e , C_S , $\bar{g}_\pi^{(0)}$, $\bar{g}_\pi^{(1)}$, \bar{d}_n^{sr} , and $C_T^{(0,1)}$.

As indicated above, the two tensor contributions depend on the same Wilson coefficient $\text{Im } C_{lequ}^{(3)}$, so these couplings differ only through the values of the nucleon form factors $g_T^{(0,1)}$. At this level of interpretation, a meaningful fit would include only one parameter rather than two distinct and independent tensor couplings. Unfortunately, we presently possess limited information on the nucleon tensor form factors $g_T^{(0,1)}$, and the theoretical uncertainties associated with existing computations are sizable. Consequently, we adopt an interim strategy until refined computations of the tensor form factors are available, retaining only $C_T^{(0)}$ in the fit. Henceforth, we denote this parameter by C_T .

III. EXPERIMENTAL STATUS AND PROSPECTS

Over the past six decades, a large number of EDM measurements in a variety of systems have provided results, all of which are consistent with zero. The most recent or best result for each system used in our analysis is presented in Table III. The results are separated into two distinct categories as indicated above: (a) paramagnetic atoms and molecules and (b) diamagnetic systems (including the neutron). Although paramagnetic systems (Cs, Tl, YbF, and ThO) are most sensitive to both the electron EDM d_e and the nuclear spin-independent component of the electron-nucleus coupling (C_S), most experimenters have presented their results as a measurement of d_e , which requires the assumption that

TABLE III. EDM results used in our analysis as presented by the authors. When d_e is presented, the assumption is $C_S = 0$, and for ThO, the C_S result assumes $d_e = 0$. We have combined statistical and systematic errors in quadrature for cases where they are separately reported by the experimenters.

System	Year/ref	Result
Paramagnetic systems		
Cs	1989 [36]	$d_A = (-1.8 \pm 6.9) \times 10^{-24}$ e cm $d_e = (-1.5 \pm 5.6) \times 10^{-26}$ e cm
Tl	2002 [9]	$d_A = (-4.0 \pm 4.3) \times 10^{-25}$ e cm $d_e = (6.9 \pm 7.4) \times 10^{-28}$ e cm
YbF	2011 [8]	$d_e = (-2.4 \pm 5.9) \times 10^{-28}$ e cm
ThO	2014 [7]	$\omega^{\text{NE}} = 2.6 \pm 5.8$ mrad/s $d_e = (-2.1 \pm 4.5) \times 10^{-29}$ e cm $C_S = (-1.3 \pm 3.0) \times 10^{-9}$
Diamagnetic systems		
^{199}Hg	2009 [5]	$d_A = (0.49 \pm 1.5) \times 10^{-29}$ e cm
^{129}Xe	2001 [37]	$d_A = (0.7 \pm 3) \times 10^{-27}$ e cm
TlF	2000 [38]	$d = (-1.7 \pm 2.9) \times 10^{-23}$ e cm
Neutron	2006 [4]	$d_n = (0.2 \pm 1.7) \times 10^{-26}$ e cm

TABLE IV. Sensitivity to d_e and C_S and the ratio $\alpha_{C_S}/\alpha_{d_e}$ for observables in paramagnetic systems based on atomic theory calculations. Ranges (bottom entry) for coefficients α_{ij} representing the contribution of each of the TVPV parameters to the observed EDM of each system. See Refs. [1,39] for Cs and Tl. For YbF, theory results are compiled in Ref. [13], and for ThO we use result from Refs. [13,18,19].

System	α_{d_e}	α_{C_S}	$\alpha_{C_S}/\alpha_{d_e}$ (e cm)
Cs	123 (100 – 138)	7.1×10^{-19} e cm (7.0 – 7.2)	5.8×10^{-21} (0.6 – 0.7) $\times 10^{-20}$
Tl	-573 (-562 – 716)	-7×10^{-18} e cm (-5 – 9)	1.2×10^{-20} (1.1 – 1.2) $\times 10^{-20}$
YbF	-1.1×10^{25} Hz/e cm (-0.9 – 1.2)	-9.2×10^4 Hz (-92 – 132)	8.6×10^{-21} (8.0 – 9.0) $\times 10^{-21}$
ThO	-5.0×10^{25} Hz/e cm (-4.0 – 5.0)	-6.6×10^5 Hz (-4.6 – 6.6)	1.3×10^{-20} (1.2 – 1.3) $\times 10^{-20}$

$C_S = 0$. As we discuss below, this assumption is not required in a global analysis of EDM results.

Diamagnetic systems, including ^{129}Xe and ^{199}Hg atoms, the molecule TlF, and the neutron, are most sensitive to purely hadronic CPV sources, as well as the tensor component of the electron-nucleus coupling C_T for atoms and molecules; however the electron EDM and C_S contribute to the diamagnetic atoms in higher order. The constraints provided by the diamagnetic systems are expected to change significantly within the next few years. Strong efforts or proposals at several laboratories foresee improving the neutron-EDM sensitivity by one or more orders of magnitude [26–31], and the EDM of ^{129}Xe by several orders of magnitude [32,33]. Most importantly, there has been significant progress in theory and towards a measurement of the EDMs of heavy atoms with octupole-deformed nuclei, i.e., in ^{225}Ra [34] and ^{221}Rn or ^{223}Rn [35]. In these systems, the nuclear structure effects are expected to enhance the Schiff moment generated by the long-range TVPV pion-exchange interaction, leading to an atomic EDM two or three orders of magnitude larger than ^{199}Hg . As we show below, an atomic-EDM measurement at the 10^{-26} e cm level will provide additional input that will significantly impact our knowledge of the TVPV hadronic parameters.

A. Constraints on TVPV couplings

From the arguments presented above, there are seven dominant effective-field-theory parameters: d_e , C_S , C_T , $\bar{g}_\pi^{(0)}$, $\bar{g}_\pi^{(1)}$, and the two isospin components of the short-range hadronic contributions to the neutron and proton EDMs, which we isolate as \bar{d}_n^{sr} and \bar{d}_p^{sr} in Eq. (2.16). We, thus, write the EDM

of a particular system as

$$d = \alpha_{d_e} d_e + \alpha_{C_S} C_S + \alpha_{C_T} C_T + \alpha_{\bar{d}_n^{\text{sr}}} \bar{d}_n^{\text{sr}} + \alpha_{\bar{d}_p^{\text{sr}}} \bar{d}_p^{\text{sr}} + \alpha_{g_\pi^0} \bar{g}_\pi^0 + \alpha_{g_\pi^1} \bar{g}_\pi^1, \quad (3.1)$$

where $\alpha_{d_e} = \partial d / \partial d_e$, etc. This can be compactly written as

$$d_i = \sum_j \alpha_{ij} C_j, \quad (3.2)$$

where i labels the system and j labels the physical contribution. The coefficients α_{ij} are provided by atomic and nuclear theory calculations and are listed in Tables IV and V for diamagnetic and paramagnetic systems, respectively. The sensitivity of the EDM to these parameters is presented as a best value and range as set forth in Ref. [1].

B. Paramagnetic systems: limits on d_e and C_S

Paramagnetic systems are dominantly sensitive to d_e and C_S ; thus for Cs, Tl, YbF, and ThO, following Ref. [13] and recalling that the experimental result is reported as a limit on the electron EDM, we model the reported electron-EDM results as

$$d_{\text{para}}^{\text{exp}} \approx d_e + \frac{\alpha_{C_S}}{\alpha_{d_e}} C_S. \quad (3.3)$$

The quantities $\alpha_{C_S}/\alpha_{d_e}$ listed in Table IV vary over a small range, i.e., from $(0.6-1.5) \times 10^{-20}$ e cm for the paramagnetic systems and from $(3-5) \times 10^{-20}$ for Hg, Xe, and TlF. We note, as pointed out in Ref. [13], that while there is a significant range of α_{d_e} and α_{C_S} from different authors, there is much less dispersion in the ratio $\alpha_{C_S}/\alpha_{d_e}$ as reflected in Table IV.

TABLE V. Coefficients for P-odd/T-odd parameter contributions to EDMs for diamagnetic systems. The $\bar{g}_\pi^{(0)}$ and $\bar{g}_\pi^{(1)}$ coefficients are based on data provided in Table VI.

System	$\partial d^{\text{exp}} / \partial d_e$	$\partial d^{\text{exp}} / \partial C_S$	$\partial d^{\text{exp}} / \partial C_T$	$\partial d^{\text{exp}} / \partial g_\pi^0$	$\partial d^{\text{exp}} / \partial g_\pi^1$
^{199}Hg	-0.014	-5.9×10^{-22}	-2×10^{-20}	-3.8×10^{-18}	0
^{129}Xe	-0.0008	$-0.014 - (-0.012)$ -4.4×10^{-23}	$(-5.9 - (-2.0)) \times 10^{-20}$ 4×10^{-21} $(4 - 6) \times 10^{-21}$	$(-27 - (-1.9)) \times 10^{-18}$ -2.9×10^{-19} $(-26 - (-1.8)) \times 10^{-19}$	$(-4.9 - 1.6) \times 10^{-17}$ -2.2×10^{-19} $(-19 - (-1.1)) \times 10^{-19}$
TlF	81	2.9×10^{-18}	1.1×10^{-16}	1.2×10^{-14}	-1.6×10^{-13}
Neutron				1.5×10^{-14}	1.4×10^{-16}

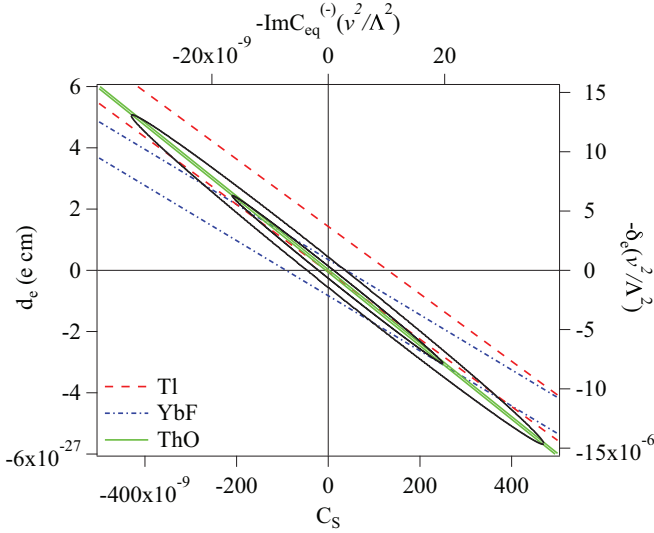


FIG. 1. (Color online) Electron EDM d_e as a function of C_S from the experimental results in Tl, YbF, and ThO. Also shown are 68% and 95% error ellipses representing the best fit for the paramagnetic systems and including $d_A(^{199}\text{Hg})$ as discussed in the text. Also shown are the constraints on the dimensionless Wilson coefficients δ_e and $\text{Im } C_{\text{eq}}^{(-)}$ times the squared scale ratio $(v/\Lambda)^2$.

In Fig. 1, we plot d_e as a function of C_S using Eq. (3.3) and experimental results for $d_{\text{para}}^{\text{exp}}$ for Tl, YbF, and ThO.

Constraints on d_e and C_S are found from a fit to the form of Eq. (3.3) for the four paramagnetic systems listed in Table III. The results using the best coefficient values are

$$d_e = (-0.4 \pm 2.2) \times 10^{-27} \text{ e cm},$$

$$C_S = (0.3 \pm 1.7) \times 10^{-7} \text{ best coefficient values.}$$

In order to account for the variation of atomic theory results we vary $\alpha_{C_S}/\alpha_{d_e}$ over the ranges presented in Table IV and find that when the $\alpha_{C_S}/\alpha_{d_e}$ are most similar,

$$d_e = (-0.3 \pm 3.0) \times 10^{-27} \text{ e cm},$$

$$C_S = (0.2 \pm 2.5) \times 10^{-7} \text{ varied coefficient values.}$$

It is in principle possible to include the diamagnetic systems, in particular ^{199}Hg , in constraining d_e and C_S . To do so, however, requires accounting for the hadronic and C_T contributions to $d_A(^{199}\text{Hg})$. As described below, the hadronic parameters and C_T are constrained by our analysis of the diamagnetic systems, though the constraints are quite weak due to the limitations of both experimental input and hadronic theory. Using the experimental result for $d_A(^{199}\text{Hg})$ combined

with the upper limits for C_T , $\bar{g}_\pi^{(0)}$ and $\bar{g}_\pi^{(1)}$, we estimate the contribution to $d_A(^{199}\text{Hg})$ from d_e and C_S , i.e.,

$$\begin{aligned} \alpha_{d_e} d_e + \alpha_{C_S} C_S &= d_A(^{199}\text{Hg}) - (\alpha_{C_T} C_T + \alpha_{\bar{g}_\pi^{(0)}} \bar{g}_\pi^{(0)} + \alpha_{\bar{g}_\pi^{(1)}} \bar{g}_\pi^{(1)}) \\ &\approx (1.2 \pm 8.0) \times 10^{-26} \text{ e cm}, \end{aligned} \quad (3.4)$$

where the coefficients α_{ij} for ^{199}Hg are given in Table V. The large numerical value follows from the uncertainties on the parameters C_T , $\bar{g}_\pi^{(0)}$, and $\bar{g}_\pi^{(1)}$ resulting from the global fit. When this additional constraint is included, the limits on d_e and C_S improve slightly due to the lever arm provided by the significantly different $\alpha_{C_S}/\alpha_{d_e}$ for ^{199}Hg compared to the paramagnetic systems with the result

$$d_e = (-0.3 \pm 2.7) \times 10^{-27} \text{ e cm},$$

$$C_S = (0.2 \pm 2.3) \times 10^{-7} \text{ including } ^{199}\text{Hg}.$$

The 68% and 95% upper limits are

$$|d_e| = < (2.7/5.4) \times 10^{-27} \text{ e cm},$$

$$|C_S| < (2.3/4.5) \times 10^{-7} \text{ (68%/95\% CL).}$$

Error ellipses representing 68% and 95% confidence interval for the two parameters d_e and C_S are presented in Fig. 1. The corresponding constraints on $\delta_e(v/\Lambda)^2$ and $\text{Im } C_{\text{eq}}^{(-)}(v/\Lambda)^2$ are obtained from those for d_e and C_S by dividing by $-3.2 \times 10^{-22} \text{ e cm}$ and -12.7 , respectively.

C. Hadronic parameters and C_T

Diamagnetic atom EDMs are most sensitive to the hadronic parameters $\bar{g}_\pi^{(0)}$ and $\bar{g}_\pi^{(1)}$ and the electron-nucleon contribution C_T . As noted above, d_e and C_S contribute to diamagnetic systems in higher order. Given that d_e and C_S are effectively constrained by the paramagnetic systems, constraints on the four free parameters C_T , $\bar{g}_\pi^{(0)}$, $\bar{g}_\pi^{(1)}$, and \bar{d}_n^{sr} are provided by four experimental results from TlF, ^{129}Xe , ^{199}Hg , and the neutron. For example, the solution using the experimental centroids and the best values for the coefficients are labeled as “exact solution” in the first line of Table VII. In order to provide estimates of the constrained ranges of the parameters, we define χ^2 for a given set of coefficients α_{ij} and a set of parameters \mathbf{C}_j :

$$\chi^2(\mathbf{C}_j) = \sum_i \frac{(d_i^{\text{exp}} - d_i)^2}{\sigma_{d_i^{\text{exp}}}^2}, \quad (3.5)$$

where d_i is given in Eq. (3.2). We then take the following steps:

TABLE VI. Best values and ranges (in parentheses) for atomic EDM sensitivity to the Schiff moment and dependence of the Schiff moments on $\bar{g}_\pi^{(0)}$ and $\bar{g}_\pi^{(1)}$ as presented in Ref. [1].

System	$\kappa_S = \frac{d}{S} \text{ (cm/fm}^3\text{)}$	$a_0 = \frac{S}{13.5\bar{g}_\pi^0} \text{ (e - fm}^3\text{)}$	$a_1 = \frac{S}{13.5\bar{g}_\pi^1} \text{ (e - fm}^3\text{)}$	$a_2 = \frac{S}{13.5\bar{g}_\pi^2} \text{ (e - fm}^3\text{)}$
TlF	-7.4×10^{-14} [20]	-0.0124	0.1612	-0.0248
Hg	$-2.8/ -4.0 \times 10^{-17}$ [40,41]	0.01 (0.005-0.05)	± 0.02 (-0.03 - 0.09)	0.02 (0.01-0.06)
Xe	$0.27/0.38 \times 10^{-17}$ [40,42]	-0.008 (-0.005 - (-0.05))	-0.006 (-0.003 - (-0.05))	-0.009 (-0.005 - (-0.1))
Ra	$-8.5(-7/ -8.5) \times 10^{-17}$ [40,43]	-1.5 (-6 - (-1))	+6.0 (4-24)	-4.0 (-15 - (-3))

TABLE VII. Values and ranges for coefficients for diamagnetic systems and the neutron. The first line is the exact solution using the central value for each of the four experimental results; the second line is the 68% CL range allowed by experiment combined with the best values of the coefficients α_{ij} ; the last three lines provide an estimate of the constraints accounting for the variations of the α_{ij} within reasonable ranges of the coefficients α_{ij} [1].

	$C_T \times 10^7$	$\bar{g}_\pi^{(0)}$	$\bar{g}_\pi^{(1)}$	\bar{d}_n^{sr} (e cm)
Exact solution	1.265	-6.687×10^{-10}	1.4308×10^{-10}	9.878×10^{-24}
Range from best values of α_{ij}	(-7.6 – 9.5)	$(-5.0 - 4.0) \times 10^{-9}$	$(-0.2 - 0.4) \times 10^{-9}$	$(-5.9 - 7.4) \times 10^{-23}$
Range from best values with $\alpha_{g_\pi^1}(\text{Hg}) = -4.9 \times 10^{-17}$	(-7.6 – 8.4)	$(-7.0 - 4.0) \times 10^{-9}$	$(0 - 0.2) \times 10^{-9}$	$(5.9 - 10.4) \times 10^{-23}$
Range from best values with $\alpha_{g_\pi^1}(\text{Hg}) = +1.6 \times 10^{-17}$	(-9.2 – 12.4)	$(-4.0 - 4.0) \times 10^{-9}$	$(-0.4 - 0.8) \times 10^{-9}$	$(-5.9 - 5.9) \times 10^{-23}$
Range from full variation of α_{ij}	(-10.8 – 15.6)	$(-10.0 - 8.1) \times 10^{-9}$	$(-0.6 - 1.2) \times 10^{-9}$	$(-12.0 - 14.8) \times 10^{-23}$

- (i) Fix d_e and C_S using paramagnetic systems only: $d_e = (-0.3 \pm 3.0) \times 10^{-27}$ e cm; $C_S = (0.2 \pm 2.5)10^{-7}$.
- (ii) Vary C_j to determine χ^2 contours for a specific set of α_{ij} . For 68% confidence and four parameters, $(\chi^2 - \chi_{\text{min}}^2) < 4.7$. (Note that $\chi_{\text{min}}^2 = 0$.)
- (iii) This procedure is repeated for values of α_{ij} spanning the reasonable ranges presented in Table V to estimate ranges C_T , $\bar{g}_\pi^{(0)}$, $\bar{g}_\pi^{(1)}$, and \bar{d}_n^{sr} .

Our estimates of the constraints are presented as ranges in Table VII. Finally, we use the ranges for C_T , $\bar{g}_\pi^{(0)}$, and $\bar{g}_\pi^{(1)}$ to determine their contribution to the EDM of ^{199}Hg and subtract to isolate the d_e/C_S contribution as described above.

IV. EXPERIMENTAL OUTLOOK AND THEORETICAL IMPLICATIONS

Anticipated advances of both theory and experiment would lead to much tighter constraints on the TVPV parameters. The disparity shown in Table VII between the ranges provided by the best values of the coefficients α_{ij} and those provided by allowing the coefficients to vary over the reasonable ranges emphasizes the importance of improving the nuclear physics calculations, particularly the Schiff moment calculations for ^{199}Hg .

On the experimental front, we anticipate the following:

- (i) Increased sensitivity of the paramagnetic ThO experiment [7].
- (ii) Improvement of up to two orders of magnitude for the neutron-EDM [26–31].
- (iii) Two to three orders of magnitude improvement for ^{129}Xe [32,33,44].
- (iv) New diamagnetic atom EDM measurements from the octupole enhanced systems ^{225}Ra [34] and $^{221}\text{Rn}/^{223}\text{Rn}$ [35].
- (v) Possible new paramagnetic atom EDM measurement from Fr [16] and Cs [45].
- (vi) Plans to develop storage-ring experiments to measure the EDMs of the proton and light nuclei ^2H and ^3He [46].

Some scenarios for improved experimental sensitivity and their impact are presented in Table VIII. In the first line we summarize the current upper limits on the parameters at the

95% CL. The remainder of the table lists the impact of one or more experiments with the improved sensitivity noted in the third column, assuming a central value of zero. Note that we do not consider a possible future proton EDM search. While every experiment has the potential for discovery in the sense that improving any current limit takes one into new territory, it is clear from Table VIII that inclusions of new systems in a global analysis may have a much greater impact on constraining the parameters than would improvement of experimental bounds in systems with current results.

For example, ThO provides such a tight correlation of d_e and C_S , as shown in Fig. 1, that narrowing the experimental upper and lower limits without improvements to the other experiments does not significantly improve the bounds on d_e and C_S . Adding a degree of freedom, such as a result in Cs or Fr, with $\alpha_{C_S}/\alpha_{d_e} \approx 1.2 \times 10^{-20}$ [13], could significantly tighten the bounds. Similarly, a result in an octupole-deformed system, e.g., ^{225}Ra or $^{221}\text{Rn}/^{223}\text{Rn}$, would add a degree of freedom and overconstrain the set of parameters C_T , $\bar{g}_\pi^{(0)}$, $\bar{g}_\pi^{(1)}$, and \bar{d}_n^{sr} . Due to the nuclear structure enhancement of the Schiff moments of such systems, their inclusion in a global analysis could have a substantial impact on the $\bar{g}_\pi^{(i)}$ as well as on C_T . In contrast, the projected 100-fold improvement in ^{129}Xe (not octupole-deformed) would have an impact primarily on C_T . In the last line of Table VIII, we optimistically consider the long-term prospects with the neutron and ^{129}Xe improvements and the octupole-deformed systems. The possibility of improvements to TIF, for example with a cooled molecular beam [47] or another molecule, will, of course, enhance the prospects.

From a theoretical perspective, it is interesting to consider the implications of the present and prospective global analysis results. Perhaps, not surprisingly, the resulting constraints on various underlying CPV sources are weaker than under the “single-source” assumption. For example, from the limit on $\bar{g}_\pi^{(0)}$ in Table I and the “reasonable range” for the hadronic matrix element computations given in Ref. [1], we obtain $|\bar{\theta}| \leq \bar{\theta}_{\text{max}}$, with

$$2 \times 10^{-7} \lesssim \bar{\theta}_{\text{max}} \lesssim 1.6 \times 10^{-6} \quad (\text{global}), \quad (4.1)$$

a constraint considerably weaker than the order 10^{-10} upper bound obtained from the neutron or ^{199}Hg EDM under the “single-source” assumption. Similarly, for the dimensionless,

TABLE VIII. Anticipated limits (95%) on P-odd/T-odd physics contributions for scenarios for improved experimental precision compared to the current limits listed in the first line using best values for coefficients in Table IV and V. We assume α_{g_1} for ^{199}Hg is 1.6×10^{-17} . For the octupole deformed systems (^{225}Ra and $^{221}\text{Rn}/^{223}\text{Rn}$) we specify the contribution of ^{225}Ra . The Schiff moment for Rn isotopes may be an order of magnitude smaller than for Ra, so for Rn one would require 10^{-26} and 10^{-27} for the fifth and sixth lines to achieve comparable sensitivity to that listed for Ra.

	Current limits (95%)		d_e (e cm)	C_S	C_T	$\bar{g}_\pi^{(0)}$	$\bar{g}_\pi^{(1)}$	\bar{d}_n^{sr} (e cm)
			5.4×10^{-27}	4.5×10^{-7}	2×10^{-6}	8×10^{-9}	1.2×10^{-9}	12×10^{-23}
System	Current (e cm)	Projected	Projected sensitivity					
ThO	5×10^{-29}	5×10^{-30}	4.0×10^{-27}	3.2×10^{-7}				
Fr		$d_e < 10^{-28}$	2.4×10^{-27}	1.8×10^{-7}				
^{129}Xe	3×10^{-27}	3×10^{-29}			3×10^{-7}	3×10^{-9}	1×10^{-9}	5×10^{-23}
Neutron/Xe	2×10^{-26}	$10^{-28}/3 \times 10^{-29}$			1×10^{-7}	1×10^{-9}	4×10^{-10}	2×10^{-23}
Ra		10^{-25}			5×10^{-8}	4×10^{-9}	1×10^{-9}	6×10^{-23}
Ra		10^{-26}			1×10^{-8}	1×10^{-9}	3×10^{-10}	2×10^{-24}
Neutron/Xe/Ra		$10^{-28}/3 \times 10^{-29}/10^{-27}$			6×10^{-9}	9×10^{-10}	3×10^{-10}	1×10^{-24}

isoscalar quark chromo-EDM, the $\bar{g}_\pi^{(0)}$ bounds imply

$$\bar{\delta}_q^{(+)} \left(\frac{v}{\Lambda} \right)^2 \lesssim 0.01, \quad (4.2)$$

where we have used the upper end of the hadronic matrix element range given in Ref. [1]. Since the quark chromo-EDMs generally arise at one-loop order and may entail strongly interacting virtual particles, we may translate the range in Eq. (4.2) into a range on the BSM mass scale Λ by taking $\bar{\delta}_q^{(+)} \sim \sin \phi_{\text{CPV}} \times (\alpha_s/4\pi)$, where ϕ_{CPV} is a CPV phase to obtain

$$\Lambda \gtrsim (2 \text{ TeV}) \times \sqrt{\sin \phi_{\text{CPV}}} \quad \text{isoscalar quark chromo-EDM (global)}. \quad (4.3)$$

We note, however that given the considerable uncertainty in the hadronic matrix element computation these bounds may be considerably weaker.⁷

For the paramagnetic systems, the present mass reach may be substantially greater. For the electron EDM, we again make the one-loop assumption for illustrative purposes, taking $\delta_e \sim \sin \phi_{\text{CPV}} \times (\alpha/4\pi)$ so that

$$\Lambda \gtrsim (1.5 \text{ TeV}) \times \sqrt{\sin \phi_{\text{CPV}}} \quad \text{electron EDM (global)}. \quad (4.4)$$

The scalar (quark) \times pseudoscalar (electron) interaction leading to a nonvanishing C_S may arise at tree level, possibly generated by exchange of a scalar particle that does not

contribute to the elementary fermion mass through spontaneous symmetry breaking. In this case, taking $\text{Im } C_{\text{eq}}^{(-)} \sim 1$ and using the bound in Table I gives

$$\Lambda \gtrsim (1300 \text{ TeV}) \times \sqrt{\sin \phi_{\text{CPV}}} \quad C_S \text{ (global)}. \quad (4.5)$$

Under the ‘‘single-source’’ assumption, these lower bounds become even more stringent.

Due to the quadratic dependence of the CPV sources on (v/Λ) , an order of magnitude increase in sensitivity to any of the hadronic parameters will extend the mass reach by roughly a factor of three. In this respect, achieving the prospective sensitivities for new systems and improvements in established systems as indicated in Table VII would lead to significantly greater mass reach. Achieving these gains, together with the refinements in nuclear and hadronic physics computations needed to translate them into robust probes of underlying CPV sources, lays out the future of EDM research in probing BSM physics.

ACKNOWLEDGMENTS

The authors thank P. Fierlinger and G. Gabrielse for useful discussions and both the Excellence Cluster Universe at the Technical University Munich and the Kavli Institute for Theoretical Physics, where a portion of this work was completed. M.J.R.M. was supported in part by US Department of Energy Contracts No. DE-SC0011095 and No. DE-FG02-08ER4153, by the National Science Foundation under Grant No. NSF PHY11-25915, and by the Wisconsin Alumni Research Foundation (WARF). T.E.C. was supported in part by the US Department of Energy Grant No. DE FG02 04 ER41331.

⁷The uncertainty for the quark CEDM is substantially larger than for those pertaining to $\bar{\theta}$ owing, in the latter case, to the constraints from chiral symmetry as discussed in Ref. [1].

- [1] J. Engel, M. J. Ramsey-Musolf, and U. van Kolck, *Prog. Part. Nucl. Phys.* **71**, 21 (2013).
 [2] T. Fukuyama, *Int. J. Mod. Phys. A* **27**, 1230015 (2012).
 [3] M. Pospelov and A. Ritz, *Ann. Phys.* **318**, 119 (2005).

- [4] C. Baker *et al.*, *Phys. Rev. Lett.* **97**, 131801 (2006).
 [5] W. C. Griffith, M. D. Swallows, T. H. Loftus, M. V. Romalis, B. R. Heckel, and E. N. Fortson, *Phys. Rev. Lett.* **102**, 101601 (2009).

- [6] D. E. Morrissey and M. J. Ramsey-Musolf, *New J. Phys.* **14**, 125003 (2012).
- [7] J. Baron *et al.* (ACME Collaboration), *Science* **343**, 269 (2014).
- [8] J. Hudson *et al.*, *Nature (London)* **473**, 493 (2011).
- [9] B. C. Regan, E. D. Commins, C. J. Schmidt, and D. DeMille, *Phys. Rev. Lett.* **88**, 071805 (2002).
- [10] K. Kumar, Z.-T. Lu, and M. J. Ramsey-Musolf, [arXiv:1312.5416](https://arxiv.org/abs/1312.5416).
- [11] Y. Li, S. Profumo, and M. Ramsey-Musolf, *J. High Energy Phys.* **08** (2010) 062.
- [12] S. Inoue, M. J. Ramsey-Musolf, and Y. Zhang, *Phys. Rev. D* **89**, 115023 (2014).
- [13] V. A. Dzuba, V. V. Flambaum, and C. Harabati, *Phys. Rev. A* **84**, 052108 (2011).
- [14] M. Jung, *J. High Energy Phys.* **05** (2013) 168.
- [15] M. Jung and A. Pich, *J. High Energy Phys.* **04** (2014) 076.
- [16] J. M. Amini, C. T. Munger, and H. Gould, *Phys. Rev. A* **75**, 063416 (2007).
- [17] C.-Y. Seng, J. de Vries, E. Mereghetti, H. H. Patel, and M. Ramsey-Musolf, *Phys. Lett. B* **736**, 147 (2014).
- [18] E. R. Meyer and J. L. Bohn, *Phys. Rev. A* **78**, 010502(R) (2008).
- [19] L. V. Skripnikov, A. N. Petrov, and A. V. Titov, *J. Chem. Phys.* **139**, 221103 (2013).
- [20] P. V. Coveney and P. G. H. Sandars, *J. Phys. B* **16**, 3727 (1983).
- [21] M. Kobayashi and T. Maskawa, *Prog. Theor. Phys.* **49**, 652 (1973).
- [22] G. 't Hooft, *Phys. Rev. Lett.* **37**, 8 (1976).
- [23] R. Jackiw and C. Rebbi, *Phys. Rev. Lett.* **37**, 172 (1976).
- [24] C. G. Callan Jr., R. F. Dashen, and D. J. Gross, *Phys. Lett. B* **63**, 334 (1976).
- [25] B. Grzadkowski, M. Iskrzynski, M. Misiak, and J. Rosiek, *J. High Energy Phys.* **10** (2010) 085.
- [26] C. A. Baker *et al.*, *J. Phys.: Conf. Ser.* **251**, 012055 (2010).
- [27] B. Lauss, *AIP Conf. Proc.* **1441**, 576 (2012).
- [28] S. K. Lamoreaux and R. Golub, *J. Phys. G: Nucl. Part. Phys.* **36**, 104002 (2009).
- [29] Y. Masuda *et al.*, *Phys. Lett. A* **376**, 1347 (2012).
- [30] I. Altarev *et al.*, *Il Nuovo Cimento C* **35**, 122 (2012).
- [31] A. P. Serebrov *et al.*, *JETP Lett.* **99**, 4 (2014).
- [32] M. V. Romalis and M. P. Ledbetter, *Phys. Rev. Lett.* **87**, 067601 (2001).
- [33] F. Kuchler, P. Fierlinger, and D. Wurm, *EPJ Web Conf.* **66**, 05011 (2014).
- [34] J. R. Guest *et al.*, *Phys. Rev. Lett.* **98**, 093001 (2007).
- [35] E. R. Tardiff *et al.*, *Hyperfine Interact.* **225**, 197 (2014).
- [36] S. A. Murthy, D. Krause, Jr., Z. L. Li, and L. R. Hunter, *Phys. Rev. Lett.* **63**, 965 (1989).
- [37] M. A. Rosenberry and T. E. Chupp, *Phys. Rev. Lett.* **86**, 22 (2001).
- [38] D. Cho, K. Sanster, and E. A. Hinds, *Phys. Rev. A* **44**, 2783 (1991).
- [39] J. S. M. Ginges and V. V. Flambaum, *Phys. Rep.* **397**, 63 (2004).
- [40] V. A. Dzuba, V. V. Flambaum, J. S. M. Ginges, and M. G. Kozlov, *Phys. Rev. A* **66**, 012111 (2002).
- [41] V. V. Flambaum, I. B. Khriplovich, and O. P. Sushkov, *Nucl. Phys. A* **449**, 750 (1986).
- [42] V. A. Dzuba, V. V. Flambaum, and P. G. Silverstrov, *Phys. Lett. B* **154**, 93 (1985).
- [43] V. Spevak, N. Auerbach, and V. V. Flambaum, *Phys. Rev. C* **56**, 1357 (1997).
- [44] I. Altarev *et al.*, *Rev. Sci. Instrum.* **85**, 075106 (2014).
- [45] F. Fang and D. S. Weiss, *Opt. Lett.* **34**, 169 (2009).
- [46] W. M. Morse, *Hyperfine Interact.* **199**, 93 (2011).
- [47] L. R. Hunter, S. K. Peck, A. S. Greenspon, S. S. Alam, and D. DeMille, *Phys. Rev. A* **85**, 012511 (2012).